



INTRABEAM SCATTERING IN ELECTRON AND PROTON STORAGE RINGS
(A REVIEW)*

A. G. Ruggiero

November 1984

*Submitted to the Proceedings of the Conference on the Interactions between Particle and Nuclear Physics, Steamboat Springs, Colorado, 1984.

INTRABEAM SCATTERING IN ELECTRON AND PROTON STORAGE RINGS (A REVIEW) *

A.G. Ruggiero
Fermi National Accelerator Laboratory

INTRODUCTION

Charged particles such as electrons and protons that are required to circulate in storage rings for long periods of time have a finite chance to collide with each other by Coulomb scattering. The phenomenon by which charged particles in the same beam, whether it is bunched or not, scatter with each other by Coulomb scattering is called Intra Beam Scattering (IBS). This phenomenon has two effects:

- (1) If the scattering angle is too large, the particles can be removed from the storage ring in one single collision event. This effect is often called the TOUSCHEK effect, sometimes the AdA effect.
- (2) When the scattering angles are sufficiently small, the particles are not necessarily lost, but the addition at random of several of these collisions will cause the beam dimensions to grow in a fashion that very similar to an expanding cloud of gas in free space. This second effect is commonly and properly called the Intrabeam scattering effect (IBS).

It is easy to understand that IBS could be a severe limitation in storage rings where high beam charge densities are required. The severity is measured by the amount of beam loss or dilution to the point where the initial required densities are lost.

The following Rutherford cross-section formula for Coulomb scattering

$$\sigma(\chi) = \frac{e^4}{m^2 u^2 \sin^4(\chi/2)} \quad (1)$$

is valid for two particles of charge e and rest mass m colliding in the center of mass frame at the relative velocity u . The scattering angle is χ . This formula is correct for the non-relativistic case.

The physics required to understand IBS is all in Eq.(1). The rest of the theory is just a mathematical formulation to estimate beam losses and enlargements. Several theories exist, with varying degree of approximations. There are basically two distinct approaches, one for electron, the other for proton beams.

ELECTRON BEAMS

The first collider for charged particles AdA, came into operation during 1961 at the Laboratori Nazionali di Frascati into Italy. Single beams had previously been stored at MURA. It could store electrons and positrons circulating in opposite directions and colliding head-on to check the monitoring reaction $e^+ + e^- \rightarrow 2\gamma$ up to an energy of 250 MeV per beam.^{1,2}

This ring is historically important for having demonstrated that charged particle beams can be stored for very long periods of time, though initially for rather modest intensities. In Frascati, during the first year of operation, it reached a capture rate of 8 electrons (or positrons) per second (!). In one particular experiment³ a total of 82 electrons (!) were stored and observed to measure the beam lifetime. Figure 1 shows the recorded beam decay versus time. The observed number of electrons is given on the vertical axis and one can actually observe individual particles being lost. The decay was due to vacuum limitations; a lifetime of about 5 hours was reached.

In 1962 the AdA ring was moved to the Laboratoire de l'Accelérateur Lineaire at Orsay in France. There, the use of the Orsay linac as injector allowed the storage of a large number of electrons and new effects were observed. The most important of these effects, the one which is relevant to this paper, is the AdA effect. The lifetime of the beam was measured and it was found to depend on the number N of particles in the beam and on the beam energy. The dependence can be fitted by

$$1/\tau = \alpha(E) N + 1/\tau_0, \quad (2)$$

where $\alpha(E)$ is a strongly energy-dependent parameter. The measurements and fitting that show the dependence with N and E are shown in Figs. 2 and 3. It may be observed that the fitting fails toward the low-energy end.

The Frascati-Orsay team immediately offered an explanation of the AdA or TOUSCHEK effect.^{4,5} This explanation was later proven correct. In the frame where the beam is at rest, the vertical and longitudinal (δq) momentum distribution widths are considerably smaller than the radial width. Coulomb scattering between two electrons can therefore lead to a transfer of radial momentum into longitudinal momentum. If the longitudinal momentum acquired is larger than

$$\Delta q = \Delta p/\gamma, \quad (3)$$

where Δp is half the momentum acceptance in the rest system of the ring (usually the height of the rf bucket), then the scattering process will cause the loss of particles. Based on this simple physical explanation, a formula was then derived for $\alpha(E)$

$$\alpha(E) = \frac{\sqrt{\pi} r_0^2 c}{hV \Delta p^2 \delta q} L(x) , \quad (4)$$

where $r_0 = 2.8 \times 10^{-13}$ cm, h is the rf harmonic number, assumed to be equal to the number of beam bunches, V is the volume of the bunch in real space, and in the limit of small x

$$L(x) = [\log \frac{1}{x} - 2.077] , \quad (5)$$

with $x = (\Delta p / Y \delta q)^2$.

Although Eq. (4) explains the measurements for $E > 100$ MeV, there was no explanation for the behaviour at lower energies. Several years later (1965) it was pointed out by H. Bruck and J. LeDuff⁶ that not two electrons scattering with each other would necessarily be lost. It is also possible that one particle could undergo a long sequence of scatterings with other particles without being lost. But of course this will cause beam growth. As the beam dimensions increase, the charge density decreases and the chance that a particle is lost by the Touschek effect reduced correspondingly. The significant change to Eq. (4) from the new theory is to allow the beam volume V to vary. This new approach explains the AdA beam lifetime observations, completely as one can see from Fig. 4.

In an electron storage ring, particles lose energy by synchrotron radiation which is then compensated back by an rf system. The beam dimensions are proportional to the beam energy spread $\delta E/E$ according to

$$\begin{aligned} \delta x &= \alpha R \sqrt{1 + \tau_x / \tau_s} \frac{\delta E}{E} \\ \delta z &= k \delta x \\ \delta s &= \frac{2R}{h} \frac{\delta E}{\Delta E_{RF}} , \end{aligned} \quad (6)$$

where α is the momentum compaction factor, R the average radius, ΔE_{RF} the RF bucket half-height, τ_x and τ_s the synchrotron-radiation damping times in the radial and longitudinal direction and k , a coupling constant which basically determines the vertical height of the beam.

The energy spread $\delta E/E$ is the result of a combination of growth opposed by radiation damping. Thus

$$(\delta E)^2 = \frac{\tau_s}{4} \left(\frac{d}{dt} \langle E^2 \rangle_Y + \frac{d}{dt} \langle E^2 \rangle_C \right) \quad (7)$$

where the first term is caused by synchrotron-radiation quantum fluctuations and is well known, and the second, as pointed out by Bruck and Le Duff, is due to multiple Coulomb scattering among the particle themselves. For the quantum fluctuations term,

$$\frac{d}{dt} \langle E^2 \rangle_Y = \frac{55}{2^3 3^{3/2}} \frac{r_o E_o c^2 h}{r^3} \gamma^7, \quad (8)$$

where r is the radius of curvature of the trajectories.

For the Coulomb scattering term,

$$\frac{d}{dt} \langle E^2 \rangle_c = \frac{N \langle \sigma u \epsilon_c^2(u) \rangle}{hV}, \quad (9)$$

where σ is the total individual Coulomb interaction cross section given by Eq. (1), and $\epsilon_c(u)$ is the energy variation for interaction for two interacting particles of transverse relative speed $2u$.

The beam volume is

$$V = (2\pi)^{3/2} n_o n_x n_z, \quad (10)$$

and the density is $\rho = N/hV$. Then

$$\langle \sigma u \epsilon_c^2(u) \rangle = \frac{2\sqrt{\pi} e r_o^2 E_o^2}{\gamma} f(x_m), \quad (11)$$

with

$$f(x_m) = \int_{x_m}^{\infty} \frac{1}{x} e^{-x} \ln \frac{x}{x_m} dx \quad (12)$$

$$\text{and } x_m = \frac{2r_o \rho^{1/3}}{\gamma^2} \quad (13)$$

Equations (7) to (13) can be evaluated numerically to find the equilibrium energy spread δE and the beam dimension growth with the help of Eq. (6).

The theory remains and is very commonly used to understand the performance of electron storage rings with a variety of applications (colliders, FEL, synchrotron radiation facilities, etc.). The Touschek effect is a serious limitation at low energies.

The dependence of the effect on the beam energy is very steep, as one can see from Figs. 3 and 4.

Modifications to the theory were added later (1966) by Pellegrini, who applied a relativistic correction and took into account the finite beam height due to synchrotron radiation also in absence of coupling. But even with these additions the general behaviour as predicted by the theory does not change.

PROTON BEAMS

From the historical point of view, the events have taken a different course for IBS in the case of proton beams. Direct evidences of such an effect has been produced only recently. There are some simple explanations for this. First, the beam-density requirements in proton storage rings were not as large as in the electron rings. Second, protons are heavier than electrons and Eq. (1) shows that scattering among particles is at a smaller angle for protons compared with electrons. If the scattering angles are smaller the chances for a particle to be lost is quite small and difficult to observe. Yet the small angle scattering will still cause a slow increase of the proton beam dimensions. Therefore, protons are less subject to the effects of intrabeam scattering than the electrons because of their mass.

A theory for intrabeam scattering for proton beams was proposed by A. Piwinski in 1974. Several features were now added that were not included in the old Touschek effect. Piwinski's theory calculates only the beam dimensions growth in all three directions. There is no mention of possible particle losses as in the old Touschek theory. In the latter, beam dimensions, as they appear in the volume V given by Eq. (10), were estimated as an average around the circumference of the ring. For this purpose, the ring lattice properties were also averaged. In reality, the beam dimensions and the velocity spreads vary from location to location, sometimes quite considerably. Piwinski has taken into account lattice variations and calculated the beam dimensions growth rates locally (see Fig. 5). An integral around the circumference of the storage ring then gives the overall growth rate.

The first evidence of IBS in a proton storage ring was found⁹ in the ISR at CERN in 1974. The experiment was performed by K. Hubner. The results are shown in Fig. 6, which gives the vertical growth rate normalized to the beam current for several ISR runs at different beam energies. Beam parameters like original dimensions were varied from one run to another. The measurements are compared with Piwinski's theory. There is a remarkable agreement at low energy, although toward large energy there are some obvious discrepancies between theory and measurements, but by no more than a factor of three. An explanation for this discrepancy has never been offered. Figure 7 gives a comparison between measurement and theory for the growth of the

momentum spread in the Hubner ISR experiment. The agreement here is excellent. Overall, these first measurements of IBS gave good confidence that the Piwinski theory was correct. One should point out that IBS did not seem to be a serious limitation to the performance of the ISR. The beam dimension growth was rather small.

Originally Piwinski wrote an expression for the factor A, (Fig. 5) with the explicit dependence on actual beam dimensions. A strong dependence of the growth rate on beam energy (γ^4) was obviously shown and for a while it was thought that IBS eventually could be relevant only at very low energies. But L. Evans and B. Zotter¹⁰ pointed out that typically several γ factors would disappear if one expressed the factor A in terms of normalized beam emittances, which are invariants. With this scaling in mind, the IBS growth rate has actually a weak dependence on the beam energy and IBS could be also important in large energy hadron collisions.

That this was the case was proven by L. Evans¹¹ in 1983 with a series of experiments on the CERN-SPS proton-antiproton collider at 270 GeV per beam. The results are shown in Fig. 8, 9a and b. The initial parameters assumed correspond to the colliding mode. The growth is very significant; it limits the beam-beam luminosity lifetime to around 16 hours despite the considerable beam energy. This new evidence makes one concerned about the IBS limitation in hadron-hadron colliders of even larger energies, like the SSC project (20 TeV x 20 TeV). We would like to emphasize again that this limitation is not caused by actual beam losses, but by the fact that the transverse beam dimensions grow to dilute the densities and therefore degrade the luminosity.

A comparison between the Piwinski theory and Evans' measurement is given in Table I. As one can see, the agreement is good. An actual beam intensity decay has been observed, but this is not caused by single scattering events like the Touschek effect for electron beams, but also by a sequence of very small scatterings which enhance the probability for a particle to be pushed slowly toward an aperture limit and then to be lost.

In contrast to the old Touschek theory, Piwinski does not make any restriction on the relative magnitude of the spreads σ_p , σ_x , and σ_z . For a proton beam, the longitudinal momentum spread can be larger than the transverse spreads, in which case there could be transfer of energy by Coulomb scattering there could be transfer of energy from the longitudinal direction to the transverse, as opposed to the case of electron beams.

In particular one can prove that (see Fig. 5)

$$f(1,1,c) = 0$$

Therefore in those lattice locations where

$$\sigma_p \sqrt{\frac{1}{\gamma^2} - \frac{D^2}{\beta_x^2}} = \sigma_x = \sigma_z, \quad (18)$$

an equilibrium is reached and the beam distribution is stable with no diffusion. In a lattice where the beam dimensions change slowly, that is where D and β_x are about constant,

$$\frac{D}{\beta_x} = \frac{1}{\gamma_t}, \quad (19)$$

where γ_t is the transition energy of the storage ring. Therefore Eq. (18) would point out that diffusion in all planes cannot be avoided for $\gamma > \gamma_t$, that is, above the transition energy, whereas for $\gamma < \gamma_t$, below transition the diffusion will exist only up to the point eq. (18) becomes to be fulfilled. It was recognized where that in reality it is not possible to satisfy eq. (18) at every location in the storage ring, because of the variations from point to point of D and β_x . Nevertheless it seems that the transition energy would still play a crucial role in the behaviour of IBS.

Toward the end of the 1970's, a CERN team, particularly K. Hubner, D. Mohl and F. Sacherer, in collaboration with Piwinski provided some refinements to the original theory to take into account large variations of the lattice parameters around the ring. The refinements have been published only recently,^{1,2} but a computer code (IBS by Hubner and Sacherer) has been available from CERN and widely used.

The major changes dealt with a more accurate version of some of the lattice function integrals, as, for instance, replacing the quantity D^2/β_x^2 in eq. (18) with

$$\frac{D^2}{\beta_x^2} \left(1 + \frac{\beta_x'^2}{4}\right) - \frac{\beta_x'}{\beta_x} DD' + D'^2, \quad (20)$$

which for $\beta_x' = D' = 0$ reduces to the original expression and shows what was missing in the original Piwinski theory. These modifications have been found to be quite significant for strong-focusing rings.

With the same intent, but a different approach based on an S-matrix formalism, Bjorken and Mtingwa^{1,3} have provided their own formulation of the theory. There is complete agreement between the two approaches and the later one represents a new way to understand the problem and is recommended to the readers.

FURTHER EXAMPLES

There are storage rings where very diluted beams of rare particles, antiprotons, are kept circulating. The function of these rings is to squeeze the beam to large phase-space densities by either stochastic or electron cooling techniques. It has been recognized that the largest density achievable depends on IBS. Let ϵ be either one of the betatron or the longitudinal emittance; then it is possible to

write an equation which describes the behaviour of ϵ with time under the effect of cooling and IBS.

$$\frac{d\epsilon}{dt} = F(N, \epsilon) + D_c(N, \epsilon) + ND_{IBS}(\epsilon), \quad (21)$$

where F is the friction force, usually proportional to ϵ , and D_c is a diffusion term introduced by the cooling system itself. Both F and D_c could depend on the beam intensity N in stochastic cooling. The last term is due to IBS. It is proportional to N and can have a strong dependence on the beam emittance itself. For a given N , it is possible to estimate an equilibrium value ϵ_∞ , which is obtained by setting the left-hand side of Eq. (21) to zero. This value represents the highest density possible with IBS taken into account since one usually gets to a point where the last term of (21) equals or predominates over the second one.

With carefully planned experiments, it has indeed been possible to verify^{1,2} that IBS plays a crucial role in the CERN-AA ring, where antiproton beams are cooled by stochastic techniques. The beam enlargement caused by IBS in this ring has been measured and compared with the prediction of the generalized Piwinski theory using the CERN computer code IBS. The agreement between experiment and theory was found to be remarkable.

Recently a lot of interest has been shown for heavy-ions colliders at relativistic and ultra relativistic energies. Consider for instance of RHIC, the project for BNL, described at this conference. Heavy ions have a very large mass, A times the mass of protons, but also a large charge, Z times the charge of an electron. The Rutherford formula has to be modified to include a factor

$$Z^4/A^2$$

For Gold (Au, $Z = 79$, $A = 197$), this is about 1000 times larger than for protons, but still 4000 times smaller than for electrons.

At the same density level, we do not expect electron-like effects like Touschek effect for heavy ions, but rather beam dimensions growth by multiple scattering as for protons, but at an accelerated rate.

REFERENCES

1. C. Bernardini et al., Il Nuovo Cimento, Vol. XVIII, N. 5, 16 Dec. 1960, page 1293.
2. C. Bernardini et al., 1961 International Conference on High Energy Accelerators, Sept. 1961, Brookhaven National Laboratory, NY, page 256.
3. C. Bernardini et al., Il Nuovo Cimento, Vol. XXIII, N. 1, 1 Jan 1962, page 201.
4. C. Bernardini et al., Phys. Rev. Letters, Vol. 10, N. 9, May 1, 1963, page 407.

5. C. Bernardini, Internat. Conf. on High Energy Accelerators, Dubna 1963, page 332.
6. H. Bruck and J. LeDuff, V Intern. Conf. on High Energy Accelerators, Frascati, 1965, page 284.
7. C. Pellegrini, Intern. Symposium on Electron Positron Storage Rings; SACLAY 1966, page IV-6-1.
8. A. Piwinski, IX International Conf. on High Energy Accelerators, Stanford, Calif. May 1974, page 405.
9. K. Hubner, IEEE Trans. on Nucl. Sci., Vol. NS-22, No. 3, June 1975, page 1416.
10. L. Evans and B. Zotter, CERN/SPS/80-15 (DI), 1980.
11. L.R. Evans, 12th Intern. Conf. on High Energy Accelerators, Fermilab, Illinois, Aug. 1983, p. 229.
12. M. Martini, CERN PS/84-9 (AA) May, 1984.
13. J.D. Bjorken and S.K. Mtingwa, Particle Accelerators, Vol. 13, p. 115, 1983.

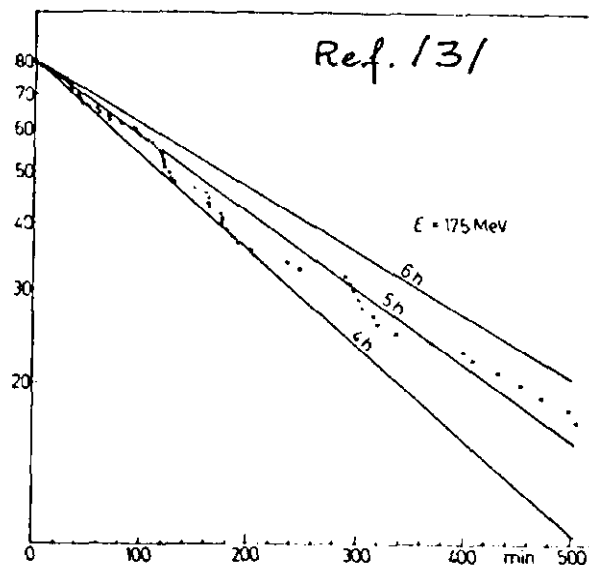


Fig. 1 Observed decay of 82 stored electrons in AdA at 175 MeV energy. Straight lines are drawn for convenience corresponding to a lifetime of 4, 5 and 6 h. Note the apparent increase of lifetime during the period of observation. This is due to a corresponding improvement of the vacuum.

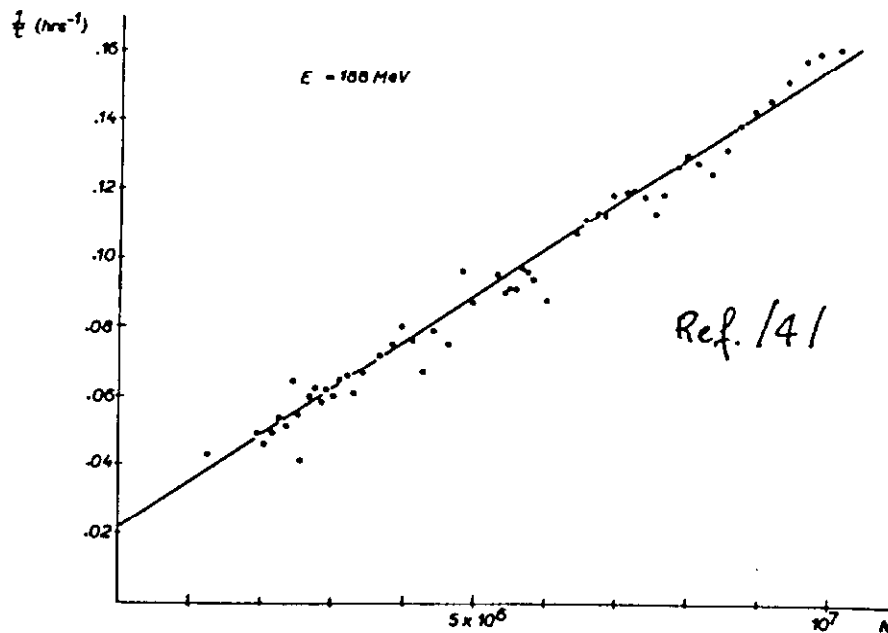


FIG. 2. Lifetime τ versus N , the number of stored particles in a beam, at the energy of 188 MeV

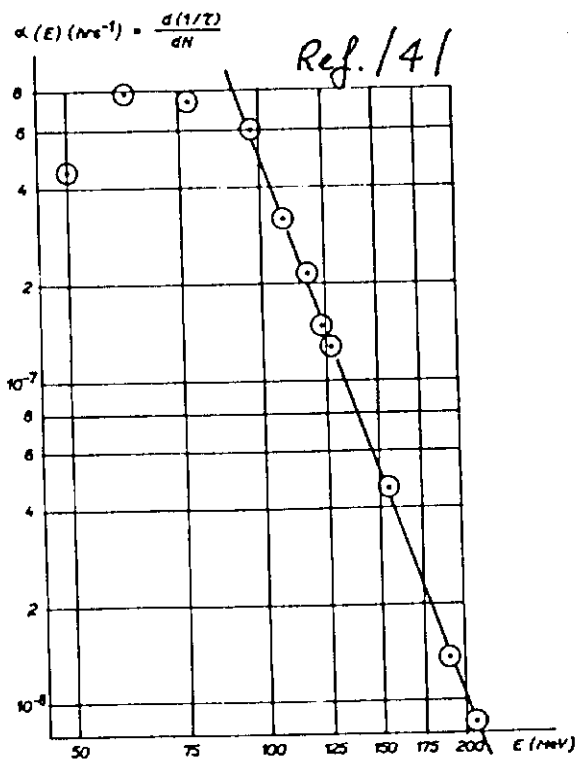


FIG. 3. Plot of the rate $\alpha(E)$, as defined in Eq. (1) of the text, versus the energy of electrons in a beam.

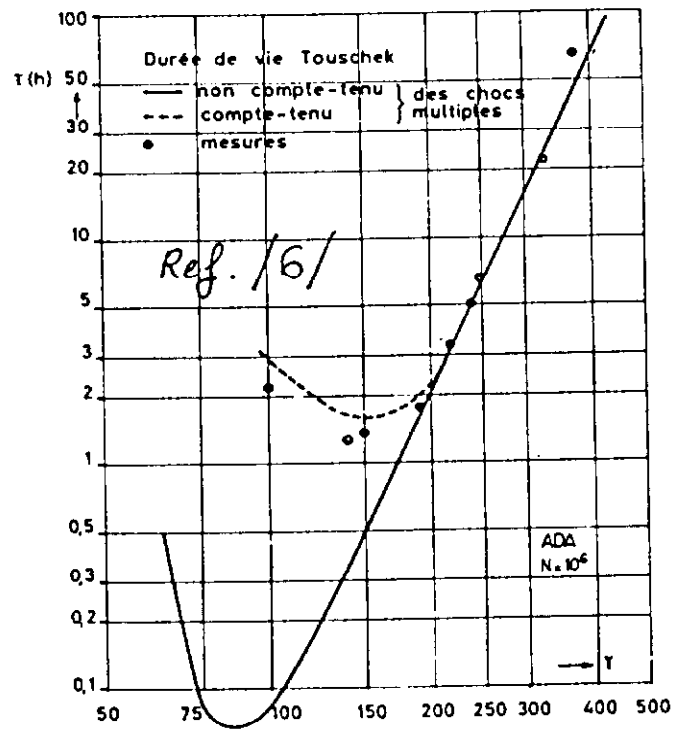


Fig. 4

Fig. 5 Main Results of Piwinski's Theory ^p

$$\frac{1}{\sigma_p} \frac{d\sigma_p}{dt} = n A \left(1 - \frac{D^2 \sigma_p^2}{\sigma_x^2}\right) f\left(\frac{\sigma_y}{\sigma_{x'}}, \frac{\sigma_y}{\sigma_{z'}}, q \sigma_y\right)$$

$$\begin{aligned} \frac{1}{\sigma_{x'}} \frac{d\sigma_{x'}}{dt} = & A \left\{ f\left(\frac{\sigma_{x'}}{\sigma_y}, \frac{\sigma_{x'}}{\sigma_{z'}}, q \sigma_{x'}\right) + \right. \\ & \left. + \frac{D^2 \sigma_p^2}{\sigma_x^2} f\left(\frac{\sigma_y}{\sigma_{x'}}, \frac{\sigma_y}{\sigma_{z'}}, q \sigma_y\right) \right\} \end{aligned}$$

$$\frac{1}{\sigma_{z'}} \frac{d\sigma_{z'}}{dt} = A f\left(\frac{\sigma_{z'}}{\sigma_y}, \frac{\sigma_{z'}}{\sigma_{x'}}, q \sigma_{z'}\right)$$

$$\sigma_y = \sigma_p \sigma_{x\beta} / \gamma \sigma_x$$

$$q = \beta \gamma \sqrt{2 \bar{b}} / r_0$$

$$\begin{aligned} f(a, b, c) = & 2 \int_0^{\sigma} \int_0^{\pi} \int_0^{2\pi} \exp \left\{ -q \left[\cos^2 \mu + (a^2 \cos^2 \nu + b^2 \sin^2 \nu) \right. \right. \\ & \left. \left. \cdot \sin^2 \mu \right] \right\} \ln(c^2 q) (1 - 3 \cos^2 \mu) \sin \mu \, d\nu \, d\mu \, d\rho \end{aligned}$$

$$A = \frac{c \sigma_0^2 N}{16 \pi \sqrt{\pi} \beta^3 \gamma^4 (\sigma_{x\beta} \sigma_{x'}) (\sigma_z \sigma_{z'}) (\sigma_z C)}$$

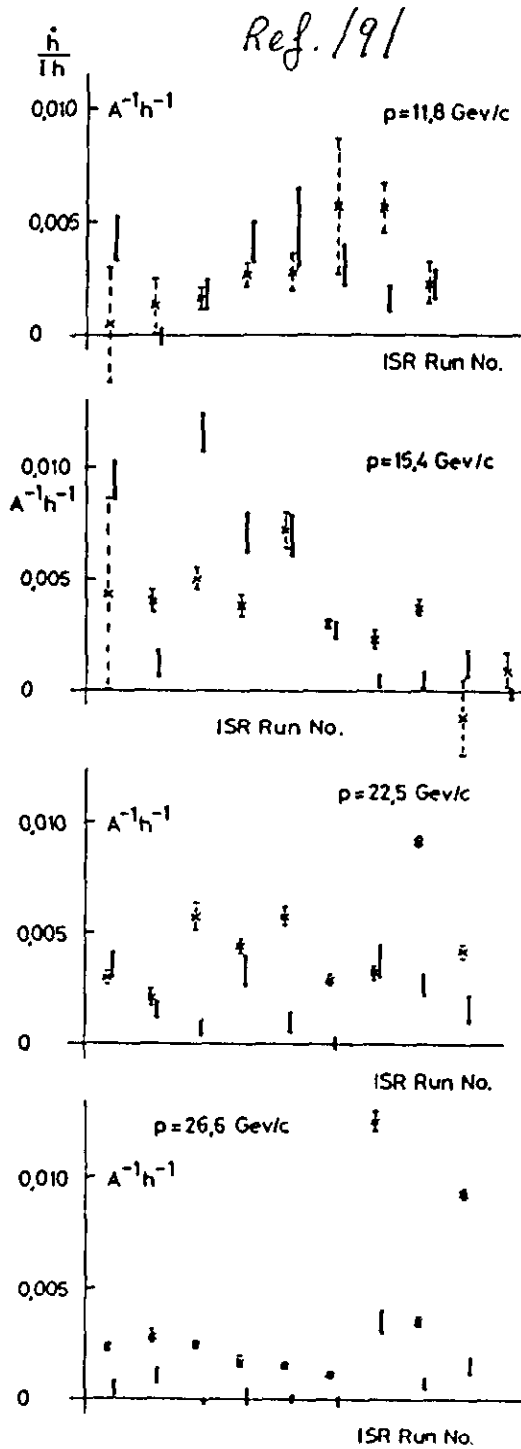


Fig. 6 - Vertical growth-rate normalized to 1 A in low current ISR runs. Dashed lines: measured rate minus multiple scattering. Full lines: calculated rate.

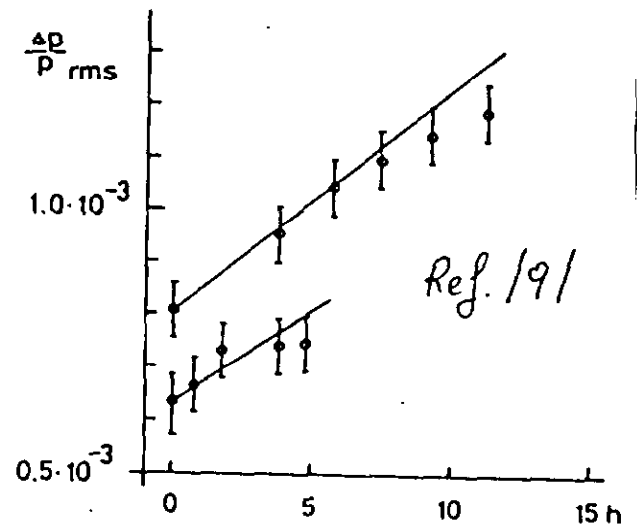


Fig. 7 - Rms momentum spread in an 1 A beam versus time at 26.6 GeV/c. Circles: measured points; full lines: computed growth.

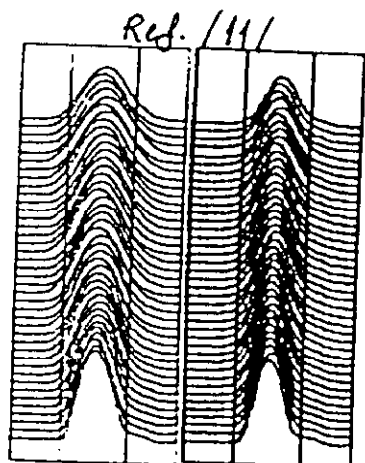


Fig. 8 a) b) Longitudinal profiles of proton a) and antiproton b) bunches at 30 minute intervals during storage.

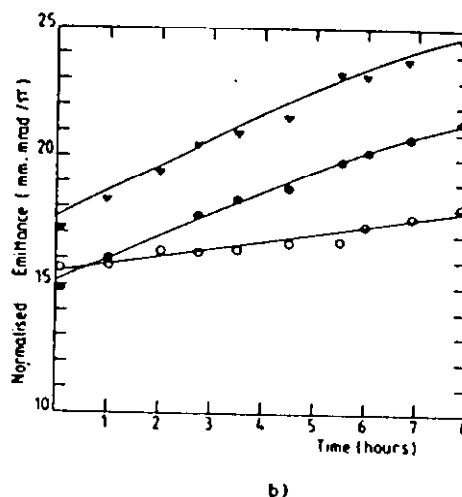
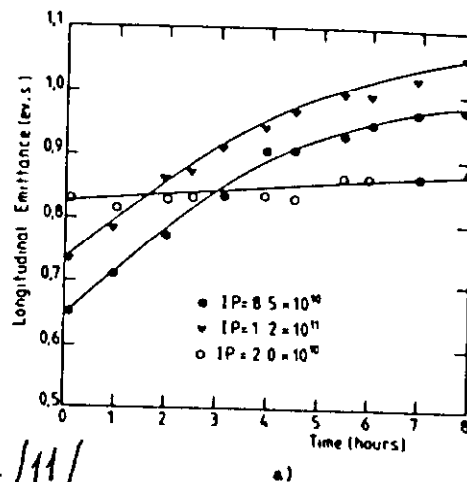


Fig. 9 Longitudinal a) and radial b) emittance growth of three proton bunches with different intensities

Ref. /11/

BUNCH	IP ($\times 10^{10}$)	$c_x \delta y / \pi$ (m.rad)	$c_z \delta y / \pi$ (m.rad)	c_p (eV.sec)	Length (nsec)	$T_x(h)$ MEASURED	$T_p(h)$ MEASURED	$T_x(h)$ THEORY	$T_p(h)$ THEORY	$T_x(h)$ MEASURED
1	8.31	14.9	17.0	0.638	2.3	17.3	11.1	20.1	16.4	31.5
2	12.39	17.2	19.7	0.730	2.44	17.5	12.7	20.7	16.5	34
3	7.01	15.6	17.0	0.829	2.63	88.7	105	114	114	194
4	13.0	18.8	21.5	0.699	2.38	24.9	15.1	22.9	16.1	67
5	13.1	18.7	21.5	1.44	3.83	47.0	-	50	84.2	127
6	3.45	13.0	14.6	1.72	3.31	52.0	-	68.6	123	68.7
7	13.9	16.6	19.0	0.683	2.35	16.3	10.0	16.4	12.4	44.7
8	11.0	16.0	18.2	1.08	3.10	26.0	50.5	29.7	39.1	60.0

Table I

Measured and theoretical growth rates under different conditions of emittance and intensity. The theoretical values were obtained by averaging over 400 lattice locations.